Mechanisms explaining the role of viscosity and post-deglutitive pharyngeal residue on in vivo aroma release: A combined experimental and modeling study

Marion M. Doyennette, Clément C. de Loubens de Verdalle, Isabelle I. Deleris, Isabelle I. Souchon, Ioan-Cristian I.-C. Trelea

Mechanisms explaining the role of viscosity and post-deglutitive pharyngeal residue on *in vivo* aroma release: a combined experimental and modeling study

M. Doyennette[*1], C. de Loubens[1], I. Déléris[1], I. Souchon[1], I. C. Trelea[1]

[1] UMR 782 Génie et Microbiologie des Procédés Alimentaires, INRA/AgroParisTech, CBAI 78850 Thiverval Grignon, France

[*] Corresponding author: Marion Doyennette, marion.doyennette@grignon.inra.fr; fax: +33 (0)1 30 81 55 97

Abstract

The objective of this study was to analyze the viscosity effect of liquid Newtonian products on aroma release, taking human physiological characteristics into account. *In vivo* release of diacetyl from glucose syrup solutions varying widely in viscosity (from 0.7 to 405 mPa s) was assessed by five panelists using Proton Transfer Reaction Mass Spectrometry (PTR-MS). The physicochemical properties of the solutions and the physiological parameters of subjects were experimentally measured. In parallel, a mechanistic model describing aroma release while eating a liquid food was developed. Model predictions based on the characteristics of the glucose syrup solution were invalidated when compared to *in vivo* measurements. Therefore, the assumption that the post-deglutitive pharyngeal residue was considerably diluted with saliva was introduced into the model. Under this hypothesis, the model gives a satisfactory prediction of the *in vivo* data. Thus, relevant properties to be considered for *in vivo* release were those of product-saliva mixes.

Keywords: Flavor release; saliva dilution; swallowing; dynamic modeling; rheology.

1. Introduction

Aroma compound release and perception determine the aromatic quality of food products and contribute to consumer choices and preferences. During consumption, flavor delivery is particularly determined by product properties (structure and composition) and individual physiology. Understanding the key mechanisms of release is of great practical interest for rational food design and formulation (Linforth & Taylor, 2000).

In the present work, the focus has been placed on the effect of matrix viscosity. This subject has already been discussed in the literature but there appears to be no consensus. On the one hand, some authors observed no effect of product viscosity on aroma release kinetics (Cook, Hollowood, Linforth & Taylor, 2003; Hollowood, Linforth & Taylor, 2002; Weel, Boelrijk, Burger, Verschueren, Gruppen, Voragen et al., 2004). These authors studied solutions viscosified with hydrocolloids. Their analysis may have been biased by the fact that the concentration of the viscosifying agent modified both rheological and physico-chemical properties. On the other hand, some authors found an impact of viscosity on aroma release (Saint-Eve, Martin, Guillemin, Semon, Guichard & Souchon, 2006). They obtained different rheological properties by a mechanical treatment that does not modify the product composition and that therefore leaves physico-chemical properties such as air/product partition coefficients unchanged (Kora, Souchon, Latrille, Martin & Marin, 2004). In that way, authors were able to uncouple rheological and physico-chemical properties in their study. Saint-Eve et al. (2006) showed a strong influence of yogurt complex viscosity on aroma release and hypothesized that these differences were due to different mechanical behaviors of the products in the mouth or in the pharynx. However, yogurts present complex rheological properties such as viscoelasticity and yield stress. These complex behaviors, leading to different experimental conditions when compared with the other studies, could explain the conflicting results.

In this context, the objective of this study was to analyze the Newtonian viscosity effects on the aroma release kinetics of the products. To this end, we measured *in vivo* aroma release kinetics by Proton Transfer Reaction Mass Spectrometry (PTR-MS) after the ingestion of glucose syrup solutions. These solutions were Newtonian liquids for which a wide range of viscosities could be obtained.

Increasing the carbohydrate concentration of the solutions increased the Newtonian viscosity but modified the air/product partition and mass transfer coefficients as well. In order to quantify these effects independently, we developed a mechanistic model that described aroma release during consumption of a liquid and semi-liquid food. Most of the model parameters related to the products or to the subjects were measured experimentally. Comparing the model predictions under different assumptions with the experimental data allowed us to understand the influence of viscosity on aroma release.

The mechanistic model describing aroma release in the present study was developed on the basis of the work described by Trelea, Atlan, Deleris, Saint-Eve, Marin & Souchon (2008). The sensitivity analysis of the previous model highlighted the parameters that have a major influence on aroma release kinetics. For example, the residual product layer thickness reduction in the pharynx accelerates the volatile compound depletion by the breath flow rate, whereas its increase induces a longer persistence effect. The breath flow rate also influences the aromatic persistence. In addition, increasing the equilibrium partition coefficient or the mass transfer coefficient increases the aroma concentration in the nasal cavity.

Most of these key parameters can be determined experimentally or evaluated from the literature. However, the residual thickness of a product is an unknown parameter that should depend both on the product viscosity and on the individual physiology. Due to the presence of saliva on the pharyngeal mucosa, two hypotheses can be formulated about the nature of this post-deglutitive pharyngeal residue. The first one considers that the initial saliva thickness in the pharynx is very thin compared to the deposited thickness of the product, or is swept out during swallowing: a pure product layer coats the mucosa. In the second hypothesis, we consider that the amount of saliva on the mucosa is large: the deposited residue layer is a mix of saliva and the product.

These two assumptions were tested successively. In order to do this, the present work was carried out in successive steps. First, a model of aroma release during ingestion was developed. In parallel, relevant physico-chemical and physiological parameters were measured using *in vitro* or *in vivo* experiments, or were calculated from the literature or experimental data. Finally, model predictions under the two hypotheses were compared to measured *in vivo* release data.

84

Nomenclature

Symbol	Unit	Parameter
A_{FAP}	cm^2	Air/product contact area in the pharynx
A_{OAP}	cm^2	Air/product contact area in the oral cavity
C_{FA}	g/cm^3	Aroma concentration present in the air in the pharynx
C_{FP}	g/cm^3	Aroma concentration present in the product in the pharynx
C^*_{FP}	g/cm^3	Aroma concentration present at the air/product interface in the pharynx
C_{NA}	g/cm^3	Aroma concentration present in the air in the nasal cavity
C_{OA}	g/cm^3	Aroma concentration present in the air in the oral cavity
C_{OP}	g/cm^3	Aroma concentration present in the product in the oral cavity
C^*_{OP}	g/cm^3	Aroma concentration present at the air/product interface in the oral cavity
e	µm	Residual product layer thickness
F_R	Number of cycles/s	Respiratory frequency
K_{AP}		Air/product partition coefficient
k_P	m/s	Mass transfer coefficient in the product layer
t_{deg}		Swallowing moment
Q_{NA}	cm^3/s	Respiratory flow rate
Q_S	cm^3/s	Salivary flow rate
V_{FA}	cm^3	Volume of air in the pharynx
V_{FP}	cm^3	Volume of the product in the pharynx
V_{lung}	cm^3	Lung volume
V_{NA}	cm^3	Volume of air in the nasal cavity
V_{OA}	cm^3	Volume of air in the oral cavity
V_{OP}	cm^3	Volume of product in the oral cavity
V_{OPres}	cm^3	Volume of residual product in the oral cavity
V_T	cm^3	Tidal volume

ϕ_{FPA}	g/s	Volatile mass flux between the product and the air in the pharynx
ϕ_{OPA}	g/s	Volatile mass flux between the product and the air in the oral cavity
τ	s	Characteristic time of the aroma release decay

2. Material and Methods

2.1. Mathematical model for *in vivo* release

2.1.1. Principle of the model

A model describing aroma compound release during liquid and semi-liquid food consumption was previously developed by Trelea et al. (2008). It is based on a physiological representation of the deglutition process as described by Buettner, Beer, Hannig & Settles (2001). A schematic representation of the various compartments involved in the modeling design, as well as their connections, is given in Fig. 1A. We considered that the oral cavity (index O), the pharynx (index F) and the nasal cavity (index N) were interconnected compartments containing product and/or air phase.

In the present study, two main simplifications were performed with the aim of eliminating parameters that have little impact on model predictions and which are difficult to determine experimentally.

The first simplification concerns the number of swallowing steps. In the original model, the product consumption process was decomposed into a series of four steps. Three of them concerned the deglutition event. However, they were very short and quite difficult to validate experimentally. Therefore, the new version of the model considers only three steps: product residence in the mouth, swallowing and release after swallowing. The swallowing step includes simultaneous contraction of the oral cavity and of the pharynx, leading to air and product expulsion, followed by relaxation and filling with fresh air. Figure 1B shows the successive steps modeled in the present work.

The second simplification of the model consisted in neglecting the aroma compound transfer resistance in the air at the gas/product interface compared to the resistance in the product.

After these model simplifications, the number of physicochemical and physiological parameters that needs to be known is reduced from 24 to 16. A comparison of the new model with the previous one shows that these simplifications do not change the predictions in any significant way.

Therefore, the model simulates the relative concentration of a specific aroma compound in the nose space of the subject. Aroma compound concentrations in all compartments (oral cavity, pharynx and nasal cavity) were calculated using mass transfer equations and mass balances. Isothermal conditions were assumed. Moreover, aroma compounds have a strong preference for the aqueous phase compared to the air, and the contact area between air and lungs is very large (~100 m^2) (Menache, Hanna, Gross, Lou, Zinreich, Leopold et al., 1997). Thus, it seems reasonable to assume that aroma compounds are quickly absorbed into the lungs. It was therefore assumed that the air coming from the trachea (i.e., the lungs) would be aroma-free. If we take a closer look at the anatomy of the nose, we can subdivide the nasal cavity into the nasal vestibule, the anterior turbinate and the posterior turbinate with different volumes and airflow rates (Wen, Inthavong, Tu & Wang, 2008). Similarly, it could be possible to take aroma compound-mucosa interactions into account. These additional phenomena were tentatively incorporated into a provisional model but were not retained in the final model, as will be explained below in the Results and Discussion section.

Moreover, concerning the presence of saliva on the pharyngeal mucosa, two different hypotheses about the nature of the bolus that coats the pharyngeal mucosa after swallowing were considered. The first one (H1) assumes that a pure product layer is deposited on the pharyngeal mucosa. The second one (H2) assumes that the product coating the pharyngeal mucosa is significantly diluted with saliva. In that case, contrarily to the first hypothesis, the physico-chemical parameters of the bolus have to be recalculated on the basis of the dilution rate.

2.1.2. Mathematical model description

We refer to the time of product introduction in mouth and the time of deglutition as t_0 and t_{deg}, respectively.

Step 1: product residence in the mouth

✓ **Product in the oral cavity**

The mouth is closed during this step and does not exchange aroma compounds with other compartments. The volume of the product in the oral cavity V_{op} increases due to dilution by saliva.

$$\frac{dV_{OP}(t)}{dt} = Q_S \quad (1)$$

The volatile mass flux ϕ_{OPA} is given by the difference between the product concentration (C_{OP}) and the interfacial concentration (C^*_{OP}):

$$\phi_{OPA}(t) = A_{OAP} \times k_P \times (C_{OP}(t) - C^*_{OP}(t)) \quad (2)$$

where k_P is the mass transfer coefficient of the aroma compound in the product.

The variation of the aroma concentration present in the product C_{OP} is due to release to the air in the mouth (transfer through the product-air interface A_{OAP}) and to dilution by saliva flow Q_S:

$$V_{OP}(t) \times \frac{dC_{OP}(t)}{dt} = -\phi_{OPA}(t) - Q_S \times C_{OP}(t) \quad (3)$$

✓ **Air in the oral cavity**

The variation of aroma concentration in the air C_{OA} is due to the volatile flux from the product in the mouth ϕ_{OPA}:

$$V_{OA} \times \frac{dC_{OA}(t)}{dt} = \phi_{OPA}(t) \quad (4)$$

✓ **Interfacial conditions**

The interfacial aroma compound concentration on the product side was calculated using the partition conditions at the interface (Cussler, 1997). Since transfer resistance on the air side was assumed to be negligible, the interfacial air concentration is the same as the bulk air concentration:

$$K_{AP} = \frac{C_{OA}(t)}{C^{*}_{OP}(t)} \quad (5)$$

where K_{AP} is the air/product partition coefficient.

Initial conditions for Step 1: product residence in the mouth

At the beginning of Step 1, the product introduced into the mouth (C_{OPini}) is the only compartment containing aroma compounds. Hence, the initial conditions are:

$$C_{OP}(t_0) = C_{OPini} \quad (6)$$

$$C_{OA}(t_0) = C_{FP}(t_0) = C_{FA}(t_0) = C_{NA}(t_0) = 0 \quad (7)$$

Step 2: Swallowing

The deglutition step is very short compared to the mouth residence step. The main modeling implication is that the transfer to the gaseous phase is negligible during deglutition.

To describe this sequence of very quick contraction and relaxation events, the following notation is used (Fig. 1B):

- t_{deg-} corresponds to the product and air status immediately before the oral and pharyngeal contraction begins. It is the end of Step 1;
- t_{deg} corresponds to the status between the end of the contraction and the subsequent relaxation of the pharynx and mouth;
- t_{deg+} corresponds to the moment just after pharynx and mouth relaxation. This is the end of Step 2 and the beginning of Step 3.

✓ **Product in the oral cavity**

After the oral cavity contraction, the residual amount of product is assumed to be equal to the usual residual amount of saliva:

$$V_{OP}(t_{\deg}) = V_{O\Pr es} \quad (8)$$

185 Since Step 2 is very short, the aroma compound concentration in the oral cavity is unchanged during
186 deglutition (negligible dilution by saliva and transfer to air):

187 $$C_{OP}(t_{\deg+}) = C_{OP}(t_{\deg}) = C_{OP}(t_{\deg-}) \quad (9)$$

188

189 ✓ **Product in the pharynx**

190 During deglutition, it is assumed under hypothesis (H1) that the saliva film in the pharynx is swept out
191 by the large amount of product coming from the mouth:

192 $$C_{FP}(t_{\deg+}) = C_{OP}(t_{\deg-}) \quad (10)$$

193 Under hypothesis (H2), only a small part of the product coming from the mouth is mixed with
194 the saliva film in the pharynx. This corresponds to the dilution factor discussed below.
195 ✓ **Air in nasal cavity, pharynx and mouth**

196 Assuming that during the contraction, the expelled air is well mixed in the mouth, pharynx and nose,
197 the intermediate aroma compound concentration in the nasal cavity, after contraction, is given by the
198 total mass divided by the total volume:

199 $$C_{NA}(t_{\deg}) = \frac{V_{OA} \times C_{OA}(t_{\deg-}) + V_{FA} \times C_{FA}(t_{\deg-}) + V_{NA} \times C_{NA}(t_{\deg-})}{V_{OA} + V_{FA} + V_{NA}} \quad (11)$$

200 After the contraction, the amount of aroma compound present in the upper airway is $V_{NA} \times C_{NA}(t_{\deg})$.
201 After relaxation, this amount is diluted by ambient air. Assuming good mixing, the final
202 concentrations will be:

203 $$C_{NA}(t_{\deg+}) = C_{FA}(t_{\deg+}) = C_{OA}(t_{\deg+}) = \frac{V_{NA} \times C_{NA}(t_{\deg})}{V_{OA} + V_{FA} + V_{NA}} \quad (12)$$

204

205

206 <u>Step 3: Release after swallowing</u>

207 The initial conditions of Step 3 are the final values of Step 2 (at t_{deg+}).

208

209 ✓ **Product in the pharynx**

The residual product in the pharynx releases aroma compounds into the adjacent air. The volatile flux ϕ_{FPA} is given by:

$$\phi_{FPA}(t) = A_{FAP} \times k_P \times (C_{FP}(t) - C^*_{FP}(t)) \quad (13)$$

The mass balance of the aroma compound in the product layer gives:

$$V_{FP} \times \frac{dC_{FP}(t)}{dt} = -\phi_{FPA}(t) \quad (14)$$

The product volume in the pharynx V_{FP} can be expressed as the product of the residual layer thickness e and the pharynx area A_{FAP}, i.e. $V_{FP} = A_{FAP} \times e$. The previous equation can be further simplified to:

$$\frac{dC_{FP}(t)}{dt} = -\frac{k_p}{e} \times (C_{FP}(t) - C^*_{FP}(t)) \quad (15)$$

✓ **Air in the pharynx**

The air in the pharynx exchanges aroma compounds with the residual product coating the pharynx walls and with the airflow Q_{NA} from the nasal cavity (inhalation) or the lungs (expiration).

$$V_{FA} \times \frac{dC_{FA}(t)}{dt} = \phi_{FPA}(t) + \begin{cases} Q_{NA}(t) \times (C_{NA}(t) - C_{FA}(t)) & \text{if } Q_{NA}(t) \geq 0 \quad \text{(inhalation)} \\ -Q_{NA}(t) \times (0 - C_{FA}(t)) & \text{if } Q_{NA}(t) < 0 \quad \text{(expiration)} \end{cases} \quad (16)$$

✓ **Air in the nasal cavity**

The concentration of aroma compounds in the nasal cavity results from a dilution with the ambient air during inhalation and with air coming from the pharynx during expiration:

$$V_{NA} \times \frac{dC_{NA}(t)}{dt} = \begin{cases} Q_{NA}(t) \times (0 - C_{NA}(t)) & \text{if } Q_{NA}(t) \geq 0 \quad \text{(inhalation)} \\ -Q_{NA}(t) \times (C_{FA}(t) - C_{NA}(t)) & \text{if } Q_{NA}(t) < 0 \quad \text{(expiration)} \end{cases} \quad (17)$$

✓ **Interfacial conditions**

Similarly to what happens in the oral cavity (Equation (5)), the interfacial air concentration in the pharynx is the same as the bulk air concentration:

$$K_{AP} = \frac{C_{FA}(t)}{C^*_{FP}(t)} \quad (18)$$

✓ **Calculation of the respiratory flow rate**

We based our calculation of the airflow rate Q_{NA} on the assumption that the volume of air inhaled and exhaled by the panelist had a sinusoidal shape. The tidal volume V_T and the respiratory frequency F_R were required for this calculation (Section 2.6 for details about this data acquisition).

The time shift ($t - t_{deg}$) was introduced to ensure that the deglutition event is always followed by expiration, as physiologically observed. This is referred to as a swallow breath.

Assuming that lung volume variation is as follows:

$$V_{lung}(t) = const + \frac{V_T}{2} \times \cos(\pi \times 2 \times F_R \times (t - t_{\deg})) \quad (19)$$

where the constant accounts for the average air volume in the lungs, the expression of Q_{NA} will be:

$$Q_{NA}(t) = \frac{dV_{lung}(t)}{dt} = -\pi \times F_R \times V_T \times \sin(\pi \times 2 \times F_R \times (t - t_{\deg})) \quad (20)$$

2.1.3. Model parameters

Model parameters can be related to the product, the consumer or the interaction between them.

1. Parameters related to the product

These parameters include the initial aroma compound concentration, the air/product partition coefficient and the mass transfer coefficient. The first parameter above is directly calculated from the product flavoring protocol (Section 2.2), and the second one is estimated *via* the non linear phase ratio variation method described in Atlan, Trelea, Saint-Eve, Souchon & Latrille (2006). The mass transfer coefficient was measured with the headspace method (Lauverjat, de Loubens, Deleris, Trelea & Souchon, 2009). Experimental protocols are described in detail in Section 2.4.

2. Parameters related to consumer anatomy and physiology

These parameters include the areas and volumes of the various compartments of the oro-nasal-pharyngeal sphere, as well as the saliva and airflow rates. Data collection protocols are described in detail in the Section 2.6.

3. Parameters related to product-consumer interaction

These parameters are the residual amounts of the product and the air/product contact areas (both in the mouth and in the pharynx). Residual product left in the mouth after swallowing was arbitrarily set to 1% of the initial volume of product in the oral cavity. The air/product contact areas of the mouth and pharynx were calculated as detailed in Appendix A. The thickness of the post-deglutitive pharyngeal residue coating the pharynx was the degree of freedom of the model. Since it only affected the part of the curve related to the persistence of aroma, it was determined so that the model fitted the decay time of the experimental curve for each panelist, product and replicate.

The effects of these parameters on model prediction were investigated and are presented in the "Results and Discussion" section.

2.2 Preparation of flavored products

Seven solutions were prepared with a glucose syrup (C*Sweet M01623, Cerestar, Europe) and mineral water (Evian). The dry matters of final solutions varied from 0 g/100 g to 70 g/100 g. All preparations presented a Newtonian behavior, i.e., viscosity was constant regardless of the shearing rate applied. Viscosities were measured with Physica MCR301 rheometer (Anton Paar Germany GmbH, Ostfildern, Germany) and were between 0.7 and 405 mPa s at 35°C. The characteristics of the solutions are summarized in Table 1. The solutions investigated in this paper were labeled according to their approximate percentage of dry matter (for example, G60 had a dry matter of 61.11g/100g). These solutions were flavored with diacetyl and ethyl hexanoate, which had been previously dissolved in 99.46% of propylene glycol (Aldrich, France). Final concentrations of diacetyl and ethyl hexanoate in the solutions studied were approximately 20 mg/L and 88 mg/L, respectively, for the *in vivo* experiments, 140 mg/L and 8.3 mg/L, respectively, for the *in vitro* determination of air/product

partition coefficients, and 1.5 mg/L and 0.85 mg/L, respectively, for the *in vitro* determination of mass transfer coefficients.

For the rest of this work, we focused on the diacetyl results. Data concerning ethyl hexanoate will be used for the validation step.

2.3. Measurement of *in vitro* and *in vivo* aroma release by Proton Transfer Reaction–Mass Spectrometry

The dynamic release of aroma compounds for *in vitro* and *in vivo* experiments was measured online using a Proton Transfer Reaction Mass Spectrometer (PTR-MS, Ionicon, Innsbruck, Austria).

The PTR-MS inlet was connected to samples or to the subject's nose via a 1/16" PEEK tube maintained at 60°C. The PTR-MS instrument drift tube was thermally controlled (Tdrift = 60°C) and operated at Pdrift = 200 Pa with a voltage set of Udrift = 600 V. Measurements were performed with the multiple ion detection mode on specific masses with a dwell time of 50 ms per mass. Diacetyl was monitored with m/z 87 (molecular ion). For *in vivo* experiments, m/z 59 (acetone) was also monitored as a breath marker, as described in Normand, Avison & Parker (2004) and Trelea et al. (2008).

In addition, masses m/z 21 (signal for $H_3{}^{18}O^+$) and m/z 37 (signal for water clusters H_2O-H_3O^+) were monitored with a dwell time of 100 ms to check the instrument performances and cluster ion formation. m/z 21 intensity was (1.34±0.51) x 10^4 cps for *in vitro* experiments and (9.46±0. 035) x 10^3 cps for *in vivo* experiments. In both cases, the ratio of intensities of m/z 37 and 21 variation was lower than 5%. These differences were considered sufficiently small to ensure accurate PTR-MS measurements. For both *in vitro* and *in vivo* measurements, a minimum of three replicates were preformed for each condition studied.

Air was sampled from the subject's nose at a flow rate of 35 cm^3/min. Nose space air was sampled *via* two inlets of a stainless nosepiece placed in both of the assessor's nostrils.

2.4. Determination of physicochemical parameters of diacetyl

2.4.1. Determination of air/product partition coefficients

The air/product partition coefficient of diacetyl K_{AP} was measured for each solution with the Phase Ratio Method using headspace gas chromatography (Ettre, Welter & Kolb, 1993). A known amount of solution was placed in vials (22.4 cm^3, Chromacol, France) and incubated at 35°C for 5 hours. After this equilibration time, 2 cm^3 of the headspace above the product was sampled and injected with an automatic HS CombiPal sampler (CTC Analytics, Switzerland) into a gas chromatograph HP (GC-FID HP6890, Germany) equipped with an HP-INNOWax polyethylene glycol semi-capillary column J&W Scientific (30 m x 0.53 mm, with a 1 µm-thick film) and a flame ionization detector. The temperatures of the gas chromatograph injector and detector (GC-FID HP6890, Germany) were both set at 250°C. The oven program was 12 min long, starting at 40°C, for 5°C/min up to 60°C, then for 10°C/min up to 120°C, and 2 min at 120°C. The carrier gas was helium (flow rate: 8.4 cm^3/min, corresponding to a 57 cm/s average velocity at 50°C). Peak areas were measured using Hewlett-Packard Chemstation integration software.

A non-linear regression was performed on the data set as described in Atlan et al. (2006). A minimum of three replicates were performed for each solution tested.

2.4.2. Determination of mass transfer coefficients

The method used for mass transfer coefficient measurements was based on two studies: the Static Equilibrium and Headspace Dilution Analysis (Marin, Baek & Taylor, 1999) and the Volatile Air Stripping Kinetic (VASK) method (Lauverjat, de Loubens, Deleris, Trelea & Souchon, 2009).

Five g of solution were poured into 134.8-cm^3 vials (three replicates/solution). The samples were left for a minimum of 12 h at 35°C to establish thermodynamic equilibrium. The headspace was then stripped by a gaseous flow at a controlled rate of 1.45 cm^3/s (Brooks Digital Mass Flow Meter, Brooks Instrument 5860s). The evolution over time of headspace concentration of these vials was measured by PTR-MS for 25 minutes. The experiment time had to be longer than four times the characteristic

time of the headspace stripping $\frac{V}{Q}$, where V is the volume of the headspace, and Q the stripping airflow rate. In fact, when the experiment time is shorter than $\frac{V}{Q}$, the headspace concentration is mainly governed by dilution with the airflow rate and not by the transfer from the product to the air. Fitting the diacetyl release model (Appendix B for detailed equations) to experimental data made it possible to determine the mass transfer coefficient of this aroma compound in the solutions.

2.5. In-nose measurements of aroma release and data processing

Five panelists (three females and two males, all Caucasian) aged between 25 and 38 years old were recruited for this study. Only the four solutions presenting the widest range of viscosities (G0, G40, G60 and G70) were investigated *in vivo*. The 10-cm^3 samples were first left at 35°C for 2 hours to allow thermal equilibrium. Panelists were then instructed to pour the sample into their mouth, keep it while they were connecting to the PTR-MS (1-2 seconds) and to then swallow. Subjects had to continue to breathe normally through the nose (and with their mouth closed) for approximately one minute, during which time the nose-space PTR-MS signal was recorded. Each experiment was repeated three times.

An additional protocol consumption was applied for G0: panelists had to suck up a mouthful of the headspace vial with a straw, swallow it and continue to breathe normally through the nose.

On the basis of data treatment observed in the literature, the aroma release curve is rarely analyzed in its entirety. In the modeling studies of Buffo, Rapp, Krick & Reineccius (2005) and Linforth et al. (2000) on aroma compound persistence in human breath, analyses were performed on the ratio between the corresponding intensities of the second and the first expirations after swallowing for each subject and each aroma compound investigated. Hodgson, Langridge, Linforth & Taylor (2005) proceeded differently and calculated the decay exponent of the maximum intensity of the second and subsequent breath peaks plotted against time (setting apart the first aroma release peak).

Figure 2 represents the data processing results of our experimental aroma release kinetics for one panelist and one solution. Each kinetic presented a sinusoidal pattern due to the cyclic shape of the breath. For clarity, we smoothed the breath-by-breath aroma release profiles by plotting a curve linking the maxima of the sinusoids (referred to as the "peak curve" in Fig. 2), including the swallow-breath peak. Then, for each product, each panelist and for the three replicates, a mean curve and an envelope curve were built based on the peak lines. This last one represents the standard deviation of the replicates and, as a result, the intra-individual variability.

In order to validate model prediction against experimental measurements, simulated data were also represented as a peak line. For ease of comparison among different release curves, the deglutition event was always synchronized at time zero.

In the "Results and Discussion" section, two main characteristics of the curves were analyzed during *in vivo*/simulation comparison: the intensity of the first peak after swallowing, and the decay time of the curve (which is representative of the aroma persistency and related to the thickness of the post-deglutitive residue in the pharynx).

2.6. Determination of physiological parameters

Volumes of oral, nasal and pharyngeal cavities were measured with the Eccovision Acoustic Rhinopharyngometer from Eccovision (Sleep Group Solutions, North Miami Beach, FL 33162). The air/product contact areas in the mouth and in the pharynx were calculated for each panelist as described in Appendix A. However, for the air/product contact area in the mouth, we only took 60% of the calculated value, since we estimated that the brief in-mouth product residence did not allow the subjects to spread the product over the full surface of the mouth before swallowing.

The volume of solution introduced into the mouth was fixed by the experimental protocol at 10 cm^3, which corresponds to a realistic "mouthful". In-mouth saliva volume was set at 1.1 cm^3 based on data from Dawes (2008), and stimulated saliva flow rate was measured for each panelist (under a parafilm stimulation).

The tidal volume of each panelist was measured with a spirometer (SpeeDyn from Dyn'R group) and the respiratory frequency was calculated from the acetone signal measured by PTRMS during the resting time preceding each experiment.

Prior to their participation in the experiments, a written consent was obtained from all participants after a full explanation of the purpose and nature of the study.

3. Results and Discussion

3.1. Experimental data

3.1.1. Air/product partition coefficients of diacetyl

Results from PRV experiments are shown in Table 2. The diacetyl air/product partition coefficient for the pure water at 35°C was 1.28 x 10^{-3}. This value is quite close to the ones obtained by Bakker, Boudaud & Harrison (1998) at 37°C, ranging between 1.16 x 10^{-3} and 1.78 x 10^{-3}. Additional values of the diacetyl partition coefficient for pure water can be found in the literature, but mostly for experiments performed at 25°C or below. By using the Arrhenius law on data obtained by Atlan et al. (2006), it is possible to calculate an activation energy of 40.7°kJ/mol and to extrapolate a partition coefficient value of 1.18x10^{-3} at 35°C, which is very close to the value found in the present work.

We can observe that the air/product partition coefficient increases with the dry matter for values greater than 5% of dry matter solution. Values range from 0.57 x 10^{-3} for G5 up to 2.5 x 10^{-3} for G70. Most of the data available in the literature are for sucrose. For example, Friel, Linforth & Taylor (2000) showed a similar trend in the air/product partition coefficient for diacetyl for a variation of sucrose concentrations. These phenomena could be explained by a loss of free water due to hydration of sugar molecules. Increasing the sucrose concentration makes the solvent character of a solution more hydrophobic. Therefore, for a hydrophilic aroma compound such as diacetyl, its affinity for the

414 product would be reduced (Nahon, Koren, Roozen & Posthumus, 1998; Nawar, 1971; Thanh,
415 Thibeaudeau, Thibaut & Voilley, 1992).
416

417 3.1.2. Mass transfer coefficients of diacetyl

418 The mass transfer coefficients calculated with the headspace dilution method are presented in Table 2.
419 They ranged between $1.1x10^{-6}$ m/s (pure water) and $3.31x10^{-8}$ m/s (G70) at 35°C. We observe a
420 decrease in the mass transfer coefficient of diacetyl with the dry matter content of the solution. Nahon,
421 Harrison & Roozen (2000) reported similar results within a range of 0 to 60% w/w of sucrose
422 concentration.
423 Marin et al. (1999) measured a mass transfer coefficient for diacetyl at 35°C of 2×10^{-6} m/s for an
424 aqueous solution. Bakker et al. (1998) found a value of 2.7×10^{-6} m/s at 37°C for pure water and
425 showed that an increase in viscosity induced a decrease in the mass transfer coefficient, similarly to
426 our work.
427
428

429 3.1.3. Physiological parameters

430 In order to make the model as accurate as possible, all of the physiological parameters (except the
431 thickness of the product layer coating the pharynx) were measured for each panelist. The variation
432 ranges of the physiological parameters are presented in Table 3.
433 We observe that all physiological parameters present a wide range of variation. For example, the
434 volumes of oral cavity, nasal cavity and pharynx obtained by rhinopharyngometry are about 37±8,
435 11±4 and 29±9 cm^3, respectively. The contact areas in the oral cavity and the pharynx are 102±14 cm^2
436 and 60±13 cm^2, respectively.
437
438

439 3.1.4. Typical experimental results

440 We observed that the aroma release curve ("single repetition" curve in Fig. 2) has a sinusoidal shape,
441 and is synchronized with breath (data not shown): when a subject exhales, he/she brings aroma to
442 his/her nasal cavity (corresponding to the rising part of the sinusoid pattern), whereas during
443 inhalation, fresh air is delivered to the nose (decreasing part of the sinusoid pattern). We can also
444 observe that the first breath peak of the aroma release is the highest and corresponds to the delivery
445 that occurs immediately after the first swallow. The aroma concentration then gradually decreases, and
446 secondary peaks are due to the continuous aroma release induced by the flavored post-deglutitive film
447 coating the pharynx, which is permanently in contact with the breath airflow.
448 Figure 3 represents the mean peak curves of aroma release for the four solutions consumed by one
449 panelist. The global shapes of the kinetics are the same, regardless of the panelist or the product.
450 However, similarly to Buffo et al. (2005) and Linforth et al. (2000), we observed differences in
451 PTRMS responses for each subject due to their physiological characteristics. Nevertheless, G0
452 presents the highest intensity for the swallow-breath peak of aroma compound release for all panelists.
453 This observation was confirmed by a statistical analysis. Since our data were not normally distributed,
454 we performed a Friedman test (non parametric) with an excel macro developed by P. Georgin et M.
455 Gouet (available online at www.AnaStats.fr) on the *in vivo* release data, normalized by the initial
456 aroma concentration in the product, to see if we could observe a solution effect. The three analyzed
457 descriptors of the kinetics were: (1) the normalized area under the curve, (2) the normalized maximum
458 intensity I_{NAmax}/C_{OPini} (first peak intensity), and (3) the decay time of the curve τ. Results show that
459 there is a product effect on the first peak intensity (level of significance 0.05). Confirming the
460 empirical observation in Fig. 3, the classification performed with a multiple comparison test
461 (Bonferroni method with a macro developed by G. Le Page, available online at www.AnaStats.fr)
462 (Table 4) shows that the first diacetyl peak for flavored pure water (G0) is significantly higher than for
463 the other solutions (G40, G60 and G70) (level of significance 0.05).
464 The normalized area under the curve and the characteristic decay time of the curve were not
465 statistically different between the glucose syrup solutions.
466
467

3.2. Parameter effects on model predictions

As mentioned in Section 2.1, the simplifications of the model were validated by comparing the kinetics obtained with the current model and the previous one with the same parameters. A sensitivity analysis of the new model was conducted.

We found that an increase in the mass transfer coefficient of the product induced an increase in the aroma concentration in the nasal cavity and a decrease in the characteristic decay time τ.

The post-deglutitive residual thickness layer in the pharynx influences the characteristic decay time of the curve τ. In fact, this time period follows the relationship:

$$\tau \propto \frac{e}{k_p} \tag{21}$$

where e is the residual thickness layer in the pharynx and k_p the mass transfer coefficient (Equation (15)). Moreover, this parameter has no influence on the height of the first aroma release peak. Last but not least, the lower the respiratory frequency is, the higher the aroma persistence will be.

3.3. Comparison of model predictions with experimental data

This section is dedicated to the comparison of model prediction with experimental data. Firstly, we verified that the aroma compound investigated in this study, i.e., diacetyl, does not specifically interact with the mucosa of the different compartments of the oro-pharyngeal sphere and the airways. Hodgson, Parker, Linforth & Taylor (2004) stated that while volatile molecules are transferred through the upper airways, they absorb to the nasal mucosa. To check the absence of mucosa interaction, panelists were asked to absorb aroma compounds either in gaseous phase or in liquid phase, as described in the "Material and Methods" section. A typical result of each type of consumption protocol is illustrated in Fig. 4. On the one hand, we observe a curve for the liquid ingestion protocol (solid line) that shows secondary aroma release peaks due to persistence phenomena. On the other hand, the aroma release after inhaling the aroma compound in gaseous phase (dotted line) has only one major peak. This shows that no significant mucosa retention occurred. This is in agreement with the

494 work of Normand et al. (2004), stating that short persistence of the aroma release (less than 1 min,
495 which is the case in our study) is considered to be mainly due to saliva coating, whereas longer
496 persistence is due to volatile adsorption in the mucosa. Therefore, introducing an additional mucosa
497 compartment into the model was unnecessary for this aroma compound.
498 Secondly, another assumption of the model that was investigated was that complex airflow in the
499 airways could have a significant effect on aroma kinetics. Tentatively, the model was implemented by
500 considering an additional "lung" compartment and/or by subdividing the nasal cavity into several
501 compartments, i.e., the nasal vestibule, the anterior turbinate and the posterior turbinate, with
502 corresponding volumes and airflow fractions (Hahn, Scherer & Mozell, 1993). It appeared that the
503 effect of these additional compartments on model predictions was minor (results not shown).
504 Therefore, we did not keep those compartments in the final version of the model.
505
506 Finally, two different hypotheses concerning the nature of the post-deglutitive residue coating the
507 pharyngeal mucosa after swallowing were developed.
508 The first hypothesis assumed that a pure product layer is deposited on the pharyngeal mucosa. In this
509 case, the air/product partition coefficients as well as the mass transfer coefficients are those obtained
510 earlier in Section 3.1.
511 The second hypothesis assumed that the product coating the pharyngeal mucosa is highly diluted with
512 saliva. In that case, the physico-chemical parameters of the bolus need to be recalculated according to
513 the dilution rate.
514 These two hypotheses will be tested and discussed in the following sections.
515

516 3.3.1. Assumption of the pure product layer (H1)

517 By fitting the model to experimental data, we found a residual thickness layer in the pharynx of
518 14.6±3.4 µm for G0, and of 2.9±1.1 µm, 2.5±1 µm, and 0.8±0.2 µm for G40, G60 and G70,
519 respectively. In their work, Wright, Hills, Hollowood, Linforth & Taylor (2003) found a thickness of
520 film saliva (which is equivalent to our post-deglutitive residue) of 55 µm for flavored aqueous

521 solutions with only 2% of sucrose (which is close to our reference G0). Their thickness value is almost
522 four times higher than ours. This difference could result from individual variability or the
523 determination method used.
524 We then observed that similarly to *in vivo* measurements (Fig. 3), simulations predicted that the
525 highest peak intensity was reached for G0 (results not shown). The second set of bars in Fig. 5 shows
526 that the model prediction for the first aroma release peak for the aqueous solution is five times higher
527 than for the glucose syrup solutions. These differences are due to the differences that we found in the
528 mass transfer coefficients for the solutions studied. However, the *in vivo* data (first set of bars) do not
529 reveal such a large gap between the aqueous and the glucose syrup solutions (which reaches between
530 58% and 83% of G0's Imax, depending on the solution and the panelist). These discrepancies between
531 experimental observations and model predictions led us to consider that the product properties
532 considered in the model (mass transfer and air/product partition coefficients) might be misevaluated
533 due to saliva dilution.
534

535 ### 3.3.2. Assumption of the product dilution by saliva (H2)

536 Under the saliva dilution hypothesis, the aroma release profile of any glucose syrup solution predicted
537 by the model is expected to be closer to the reference solution (G0), as observed *in vivo*, because the
538 physico-chemical properties of the newly formed mixtures would be closer to the properties of water.
539 It is difficult to check this assumption *in situ* and, more specifically, to determine the quantity of saliva
540 present in the pharyngeal junction, as well as the amount of product left in the pharynx after
541 swallowing. Therefore, in order to validate this assumption, additional simulations were performed
542 and compared to *in vivo* data. Since the sensitivity analysis of the model showed that the residual
543 thickness layer does not have an impact on the first peak intensity of aroma release, we fixed this
544 parameter to the averaged value found for G0, i.e., 14.6 µm. After several tests, a common dilution
545 factor was determined for all solutions such that the model predictions fit the *in vivo* release data.
546 Physico-chemical parameters for dilutions not present in Table 2 were interpolated with the formulas
547 indicated below Table 2.

548 The dilution factor was selected to keep the ratio “Intensity of the first peak for the investigated
549 solution”/“Intensity of the first peak for G0” as close as possible to *in vivo* experimental observations.
550 Results presented in Fig. 5 (first versus last series of bars in the chart) showed that it was possible to
551 find a common dilution factor that reproduces the intensity ratios observed *in vivo*.
552 Results indicated that all glucose syrup solutions were highly diluted in the pharynx (by a factor of
553 10).
554 We validated the saliva dilution assumption with an additional aroma compound, ethyl hexanoate.
555 This molecule was chosen for its hydrophobicity, in contrast to diacetyl. Similarly to diacetyl, the
556 absence of retention by mucosa was checked. Since the two molecules were investigated together, we
557 performed simulations with the same residual thickness layer and with the same dilution factor that
558 was previously determined with diacetyl. Due to the introduction of the dilution factor, the physico-
559 chemical parameters of ethyl hexanoate in the glucose syrup solutions, G0, G5, G10 and G20, were
560 measured. On the basis of the results presented in Table 5, we can observe that the air/product
561 partition coefficient values for the three glucose syrup solutions are all higher than G0, but very close
562 to each other. For the mass transfer coefficient, we observe an opposite trend: the three glucose syrup
563 solutions values are lower than G0, but also close to each other. Similarly to the diacetyl,
564 interpolations of the experimental points were necessary to perform the simulations. For both the
565 air/product partition and mass transfer coefficients, we decided to use a linear regression between G0
566 and G5, and to calculate an averaged value between G5 and G20.
567 Comparison of the ratios “Intensity of the first peak for the investigated solution”/“Intensity of the first
568 peak for G0” between *in vivo* experiments and model predictions for ethyl hexanoate are presented in
569 Fig. 6. They show that the model provides a satisfactory prediction for all solutions under the saliva
570 dilution assumption, given the wide range of experimental variability (standard deviation bars on Fig.
571 6).
572
573 These results lead to the conclusion that the viscosity of the initial product has a limited effect on
574 aroma release for products with Newtonian properties within the wide range of viscosities studied, and
575 confirm the results of Hollowood et al. (2002). The combined modeling and experimental approach

576 conducted in this work suggests a possible explanation for this limited effect: viscous solutions are
577 highly diluted by saliva during the swallowing step and the relevant properties are those of relatively
578 similar product-saliva mixtures.
579
580

581 3.4. Conclusions

582 This work aimed at studying the influence of food viscosity on flavor release during ingestion of a
583 liquid food. The originality of this study was the combination of experimental and modeling
584 approaches that allowed us to gain insights into the aroma compound release mechanisms, based on
585 the example of the diacetyl release from glucose syrup solutions. When considering the consumption
586 of a liquid product, it can be assumed that the saliva dilution is relatively low due to the short
587 residence time in the mouth. Therefore, the hypothesis that a pure product layer was deposited on the
588 pharynx walls after ingestion of a liquid food was stated at first. This assumption was invalidated by
589 the comparison of model predictions to *in vivo* measurements. This result led us to consider the
590 dilution of the product during swallowing. This new hypothesis, stating that the film coating the
591 pharyngeal walls was a mixture of saliva and product, provided predictions compatible with
592 experimental observations for the aroma compound investigated (diacetyl). Simulations showed that
593 the dilution factors by saliva determined were quite similar, regardless of the initial dry matter of the
594 solution: approximately 10% of the initial solution was kept in the final diluted mixture. With these
595 dilution factors, we tentatively extended the model to a highly hydrophobic molecule (ethyl
596 hexanoate) with satisfactory results.
597 The formulated hypothesis has to be further confirmed based on the study of the release of other
598 aroma compounds with different physico-chemical characteristics. In parallel, work is in progress on
599 the pharynx mucosa coating to increase the understanding of these phenomena based on a mechanical
600 approach. Combining mechanical and mass transfer studies should help us to gain new insights into
601 the complex phenomena of *in vivo* aroma compound release.
602
603

604 # Acknowledgements

605 The authors gratefully acknowledge the French National Research Agency (ANR) project
606 "SensInMouth" for financial support.

607

608

References

Atlan, S., Trelea, I. C., Saint-Eve, A., Souchon, I. & Latrille, E. (2006). Processing gas chromatographic data and confidence interval calculation for partition coefficients determined by the phase ratio variation method. *Journal of Chromatography A, 1110*(1-2), 146-155.

Bakker, J., Boudaud, N. & Harrison, M. (1998). Dynamic release of diacetyl from liquid gelatin in the headspace. *Journal of Agricultural and Food Chemistry, 46*(7), 2714-2720.

Buettner, A., Beer, A., Hannig, C. & Settles, M. (2001). Observation of the swallowing process by application of videofluoroscopy and real-time magnetic resonance imaging-consequences for retronasal aroma stimulation. *Chemical Senses, 26*(9), 1211-1219.

Buffo, R. A., Rapp, J. A., Krick, T. & Reineccius, G. A. (2005). Persistence of aroma compounds in human breath after consuming an aqueous model aroma mixture. *Food Chemistry, 89*(1), 103-108.

Cankurtaran, M., Celik, H., Coskun, M., Hizal, E. & Cakmak, O. (2007). Acoustic rhinometry in healthy humans: Accuracy of area estimates and ability to quantify certain anatomic structures in the nasal cavity. *Annals of Otology Rhinology and Laryngology, 116*(12), 906-916.

Cheng, K. H., Cheng, Y. S., Yeh, H. C. & Swift, D. L. (1997). Measurements of Airway Dimensions and Calculation of Mass Transfer Characteristics of the Human Oral Passage. *Journal of Biomechanical Engineering, 119*(4), 476-482.

Collins, L. M. C. & Dawes, C. (1987). The Surface Area of the Adult Human Mouth and Thickness of the Salivary Film Covering the Teeth and Oral Mucosa. *Journal of dental research, 66*(8), 1300-1302.

634 Cook, D. J., Hollowood, T. A., Linforth, R. S. T. & Taylor, A. J. (2003). Oral shear stress
635 predicts flavour perception in viscous solutions. *Chemical Senses, 28*(1), 11-23.
636 Cussler, E. L. (1997). *Diffusion: Mass Transfer in Fluid Systems*. (2ème édition ed.).
637 Cambridge: University Press.
638 Dawes, C. (2008). Salivary flow patterns and the health of hard and soft oral tissues. *J Am*
639 *Dent Assoc, 139 Suppl*, 18S-24S.
640 Elert, G. (2009). Volume of Human Lungs. In).
641 Engelen, L., de Wijk, R. A., Prinz, J. F., van der Bilt, A. & Bosman, F. (2003). The relation
642 between saliva flow after different stimulations and the perception of flavor and
643 texture attributes in custard desserts. *Physiology & Behavior, 78*(1), 165-169.
644 Ettre, L., Welter, C. & Kolb, B. (1993). Determination of gas-liquid partition coefficients by
645 automatic equilibrium headspace-gas chromatography utilizing the phase ratio
646 variation method. *Chromatographia, 35*(1), 73-84.
647 Friel, E. N., Linforth, R. S. T. & Taylor, A. J. (2000). An empirical model to predict the
648 headspace concentration of volatile compounds above solutions containing sucrose.
649 *Food Chemistry, 71*, 309-317.
650 Hahn, I., Scherer, P. W. & Mozell, M. M. (1993). Velocity profiles measured for airflow
651 through a large-scale model of the human nasal cavity. *J Appl Physiol, 75*(5), 2273-
652 2287.
653 Hodgson, M., Langridge, J. P., Linforth, R. S. T. & Taylor, A. J. (2005). Aroma release and
654 delivery following the consumption of beverages. *Journal of Agricultural and Food*
655 *Chemistry, 53*(5), 1700-1706.
656 Hodgson, M., Parker, A., Linforth, R. S. & Taylor, A. J. (2004). In vivo studies on the long-
657 term persistence of volatiles in the breath. *Flavour and Fragrance Journal, 19*(6),
658 470-475.

659 Hollowood, T. A., Linforth, R. S. T. & Taylor, A. J. (2002). The effect of viscosity on the
660 perception of flavour. *Chemical Senses, 27*(7), 583-591.
661 Kora, E. P., Souchon, I., Latrille, E., Martin, N. & Marin, M. (2004). Composition rather than
662 viscosity modifies the aroma compound retention of flavored stirred yogurt. *Journal of*
663 *Agricultural and Food Chemistry, 52*(10), 3048-3056.
664 Lauverjat, C., de Loubens, C., Deleris, I., Trelea, I. C. & Souchon, I. (2009). Rapid
665 determination of partition and diffusion properties for salt and aroma compounds in
666 complex food matrices. *Journal of Food Engineering, 93*(4), 407-415.
667 Linforth, R. & Taylor, A. J. (2000). Persistence of Volatile Compounds in the Breath after
668 Their Consumption in Aqueous Solutions. *Journal of Agricultural and Food*
669 *Chemistry, 48*(11), 5419-5423.
670 Marieb, E. N. & Hoehn , K. (2008). *Human Anatomy & Physiology* (7th ed.): Benjamin-
671 Cummings Publishing Company.
672 Marin, M., Baek, I. & Taylor, A. J. (1999). Volatile Release from Aqueous Solutions under
673 Dynamic Headspace Dilution Conditions. *Journal of Agricultural and Food*
674 *Chemistry, 47*(11), 4750-4755.
675 Menache, M. G., Hanna, L. M., Gross, E. A., Lou, S. R., Zinreich, S. J., Leopold, D. A.,
676 Jarabek, A. M. & Miller, F. J. (1997). Upper respiratory tract surface areas and
677 volumes of laboratory animals and humans: Considerations for dosimetry models.
678 *Journal of Toxicology and Environmental Health, 50*(5), 475-506.
679 Nahon, D. F., Harrison, M. & Roozen, J. P. (2000). Modeling Flavor Release from Aqueous
680 Sucrose Solutions, Using Mass Transfer and Partition Coefficients. *Journal of*
681 *Agricultural and Food Chemistry, 48*(4), 1278-1284.

682 Nahon, D. F., Koren, P., Roozen, J. P. & Posthumus, M. A. (1998). Flavor release from
683 mixtures of sodium cyclamate, sucrose, and an orange aroma. *Journal of Agricultural*
684 *and Food Chemistry, 46*(12), 4963-4968.
685 Nawar, W. W. (1971). Some variables affecting composition of headspace aroma. *Journal of*
686 *Agricultural and Food Chemistry: 19 (6) 1057-1059, 19*(6), 1057-1059.
687 Normand, V., Avison, S. & Parker, A. (2004). Modeling the kinetics of flavour release during
688 drinking. *Chemical Senses, 29*(3), 235-245.
689 Palsson, B., Hubbell, J. A. & Plonsey, R. (2003). *Tissue Engineering* CRC Press.
690 Saint-Eve, A., Martin, N., Guillemin, H., Semon, E., Guichard, E. & Souchon, I. (2006).
691 Flavored yogurt complex viscosity influences real-time aroma release in the mouth
692 and sensory properties. *Journal of Agricultural and Food Chemistry, 54*(20), 7794-
693 7803.
694 Sherwood, L. (2006). *Fundamentals of Physiology: A Human Perspective (p.380)*: Thomson
695 Brooks/Cole.
696 Thanh, M. L., Thibeaudeau, P., Thibaut, M. A. & Voilley, A. (1992). Interactions between
697 volatile and non-volatile compounds in the presence of water. *Food Chemistry: 43 (2)*
698 *129-135, 43*(2), 129-135.
699 Tortora, G. J. & Anagnostakos, N. P. (1990). *Principles of Anatomy and Physiology (p.707)*
700 (6th edition ed.): New York: Harper-Collins.
701 Trelea, I. C., Atlan, S., Deleris, I., Saint-Eve, A., Marin, M. & Souchon, I. (2008).
702 Mechanistic mathematical model for in vivo aroma release during eating of semiliquid
703 foods. *Chemical Senses, 33*(2), 181-192.
704 Weel, K. G. C., Boelrijk, A. E. M., Burger, J. J., Verschueren, M., Gruppen, H., Voragen, A.
705 G. J. & Smit, G. (2004). New device to simulate swallowing and in vivo aroma release

in the throat from liquid and semiliquid food systems. *Journal of Agricultural and Food Chemistry, 52*(21), 6564-6571.

Wen, J., Inthavong, K., Tu, J. & Wang, S. M. (2008). Numerical simulations for detailed airflow dynamics in a human nasal cavity. *Respiratory Physiology & Neurobiology, 161*(2), 125-135.

Wright, K. M. & Hills, B. P. (2003). Modelling flavour release from a chewed bolus in the mouth: Part II. The release kinetics. *International Journal of Food Science & Technology, 38*, 361-368.

Wright, K. M., Hills, B. P., Hollowood, T. A., Linforth, R. S. T. & Taylor, A. J. (2003). Persistence effects in flavour release from liquids in the mouth. *International Journal of Food Science & Technology, 38*(3), 343-350.

Xue, S. A. & Hao, J. P. G. (2006). Normative standards for vocal tract dimensions by race as measured by acoustic pharyngometry. *Journal of Voice, 20*(3), 391-400.

Figure legends

Figure 1. A. Schematic representation of the nasal cavity, pharynx and oral cavity as interconnected reactors. B. Chronological steps of the consumption of a semi-liquid food.

Figure 2. Example of data processing for *in vivo* aroma release experiments (solution G0, with 16.5mg/L of diacetyl). Dotted line: diacetyl intensity signal recorded by PTR-MS. For clarity, only one single replicate is shown. Solid line: peak curve of the shown replicate. Bold line: mean of the three peak curves for the three replicates of the experiment. Gray area: envelope of the peak curves for the three replicates.

Figure 3. Example of *in vivo* diacetyl release for the four Newtonian solutions (panelist 1). Representation of the mean peak curves.

Figure 4. Example of *in vivo* diacetyl release during two consumption protocols. Solid line: ingestion of aromatized solution; dotted line: aspiration of aromatized air.

Figure 5. “Imax of a solution/Imax of G0” ratios for diacetyl: comparison of experimental data with the model simulations under the “pure product layer (H1)” and the “saliva dilution (H2)” assumptions.

Figure 6. “Imax of a solution/Imax of G0” ratios for ethyl hexanoate: comparison of experimental data with the model simulations under the “saliva dilution (H2)” assumption.

Tables

Table 1. Characteristics of the analyzed glucose syrup solutions.

Solutions	Dry Matter (g/100g)	Viscosity at 35°C (mPa s)
G0	0.00	0.7
G5	5.13±0.19	0.8
G10	8.99±0.30	1.1
G20	20.19±0.73	1.5
G40	45.94±1.70	7.6
G60	61.11±1.19	25.0
G70	75.68±2.65	405.0

754 Table 2. Diacetyl air/product partition coefficient (K_{ap}) and mass transfer coefficient (k_p) as a function
755 of the dry matter content for Newtonian glucose syrup solutions at 35°C.
756

Solutions	K_{ap} (g/g)† x10^{-4}	k_p (m/s)‡ x10^{-7}
G0	12.84±3.11	11.03±3.9
G5	5.72±2.21	4.26±2.18
G10	6.78±3.27	4.50±2.85
G20	4.59±3.97	2.50±2.48
G40	7.88±4.37	1.94±1.34
G60	11.69±4.28	1.24±0.48
G70	25.12±4.97	0.33±0.07

757
758 †For G10, G20, G60, 3 replicates were performed. For G0, G5, G30, G40 and G70, 6 replicates were
759 performed
760 ‡Between 3 and 9 replicates were preformed for each solution
761 For Diacetyl air/product partition coefficient (K_{ap}), the following second-degree polynomial regression
762 curve fits the data ($R^2 = 0.94$) and was used for interpolation:

763 $$K_{ap} = 8.69 \times 10^{-7} \times C_g^2 - 5.036 \times 10^{-5} \times C_g + 10.55 \times 10^{-4}$$

764 where C_g is the total carbohydrate concentration in g/100g.

765 For Diacetyl mass transfer coefficient (k_p), the following non-linear regression (exponential type) fits
766 the data ($R^2 = 0.88$) and was used for interpolation:

767 $$\log(k_p) = -6.1549 - 0.0367 \times C_g$$

768 where Cg is the total carbohydrate concentration in g/100g.

769 Error bars on the mass transfer coefficient take into account the uncertainties of the air/solution
770 partition coefficients.

771

772 Table 3. Physiological parameter values

773

	Unit	Mean value/range of variation†	Data source	Reference	Value from the literature
Oral cavity Volume	cm^3	30-45	Rhinopharyngometry	(Xue & Hao, 2006)	32.95±6.10
Nasal cavity volume	cm^3	4-14	Rhinopharyngometry	(Cankurtaran, Celik, Coskun, Hizal & Cakmak, 2007)	9.11±0.71‡
Pharynx volume	cm^3	20-45	Rhinopharyngometry	(Xue & Hao, 2006)	29.65±6.10
Residual product thickness in the pharynx	µm	0.8-14.6	Degree of freedom of the model (case of the pure product layer hypothesis)	(Wright & Hills, 2003)	$55x10^{-3}$
Salivary flow rate	cm^3/s	$3x10^{-2}$-$4.7x10^{-2}$	Standard protocol (parafilm stimulation)	(Engelen, de Wijk, Prinz, van der Bilt & Bosman, 2003) (Dawes, 2008)	Less than $3.3x10^{-2}cm^3/s$; $1.5x10^{-2}$-$2.2\ x10^{-2}cm^3/s$ (parafilm stimulation)
In-mouth saliva volume	cm^3	1.1	Literature	(Dawes, 2008)	1.1/0.8 (before/after swallowing)
In-mouth air/product contact area	cm^2	81-120	Calculated (Appendix A)	(Collins & Dawes, 1987)	214.7±12.9
Pharynx air/product contact area	cm^2	54-81	Calculated (Appendix A)	(Normand, Avison & Parker, 2004)	33
Tidal volume	cm^3	470-1460	Spirometry	(Palsson, Hubbell & Plonsey, 2003) (Elert, 2009)	390-500
Respiratory frequency	Number of cycles/ min	11.5-19.5	Ion 59 signal (PTR-MS)	(Tortora & Anagnostakos, 1990) (Sherwood, 2006) (Marieb & Hoehn 2008)	12-20

774

775

† Values of parameters measured for panelists

‡ sum of the volumes of the nasal valve, the lower and the middle turbinate

776

777 Table 4. Statistical analysis of *in vivo* diacetyl release curves

778

Solutions	I_{NAmax}/C_{OPini} (10^5cps/ppb)
G0	1.53 A
G40	1.24 AB
G60	0.99 B
G70	0.85 B

779

780 Each letter corresponds to a classification group performed with Bonferroni method (significance

781 level=0.05).

782

783

784 Table 5. Physicochemical characteristics of glucose syrup solutions aromatized with ethyl hexanoate

785

Solutions	Air/product partition coefficient (g/g) $x10^{-1}$	Mass transfer coefficient (m/s) $x10^{-6}$
G0	0.82±0.17	8.74±1.63
G5	1.30±0.51	5.46±1.84
G10	1.22±0.30	4.27±0.75
G20	1.33±0.56	5.29±2.07

786

787

788

APPENDIX A

Calculation of the area of the mouth and the pharynx

The rhinopharyngometer is an acoustic device that gives a series of cross-section areas of the upper respiratory tract, at various depths, starting from the panelist's front teeth.

The value of interest here is the lateral area of the respiratory tract. It was calculated by assuming that cross-sections are ellipses with a known eccentricity. The eccentricity was graphically estimated from a study of the measurements of airway dimensions of the human oral passage done by Cheng, Cheng, Yeh & Swift (1997).

$$Area = \sum Perimeter(h)\Delta h \quad \text{(A.1)}$$

where *dh* is the distance between two successive measurements of cross-sectional areas with the rhinopharyngometer (0.43 cm).

and:

$$Perimeter(h) = \pi \times [3 \times (a+b) - \sqrt{(3a+b) \times (a+3b)}] \quad \text{(A.2)}$$

$$S = \pi \times a \times b \quad \text{(A.3)}$$

where *S* is the cross-sectional area measured at a given distance, *a* the major radius and *b* the minor radius.

Given $k = \frac{a}{b}$ as the ratio between the two radii, we obtain:

$$a = \sqrt{\frac{S \times k}{\pi}} \quad \text{(A.4)}$$

where k = 7.4 for the mouth, 1.25 for the oropharynx and 1 for the hypopharynx.

The total area of a compartment is therefore the sum of all intermediate areas that have been calculated within the limit of the compartment considered.

APPENDIX B

Model for the determination of the Mass Transfer Coefficient

In the Volatile Air Stripping Kinetic (VASK) method (Lauverjat, de Loubens, Deleris, Trelea & Souchon, 2009), the product containing the volatile compound is equilibrated with the headspace air in a closed flask. At time t=0, the headspace is stripped with a constant airflow, and the volatile compound concentration in the outlet air is continuously measured by PTR-MS.

The volatile concentrations in the product and in the headspace are given by:

$$V_p \times \frac{dC_p}{dt} = -A \times k_p \times (C_p - \frac{C_a}{K_{ap}}) \quad \text{(B.1)}$$

$$V_a \times \frac{dC_a}{dt} = A \times k_p \times (C_p - \frac{C_a}{K_{ap}}) - C_a \times Q \quad \text{(B.2)}$$

where:

V_p and V_a are the volume of the liquid product and of the air, respectively.

A is the contact area between the air and the product.

Q is the air flow rate stripping the headspace.

C_p and C_a are the concentration of aroma in the product and in the air, respectively.

The mass transfer coefficient (k_p) is determined by fitting the air concentration predicted by the model to the PTR-MS measurements.

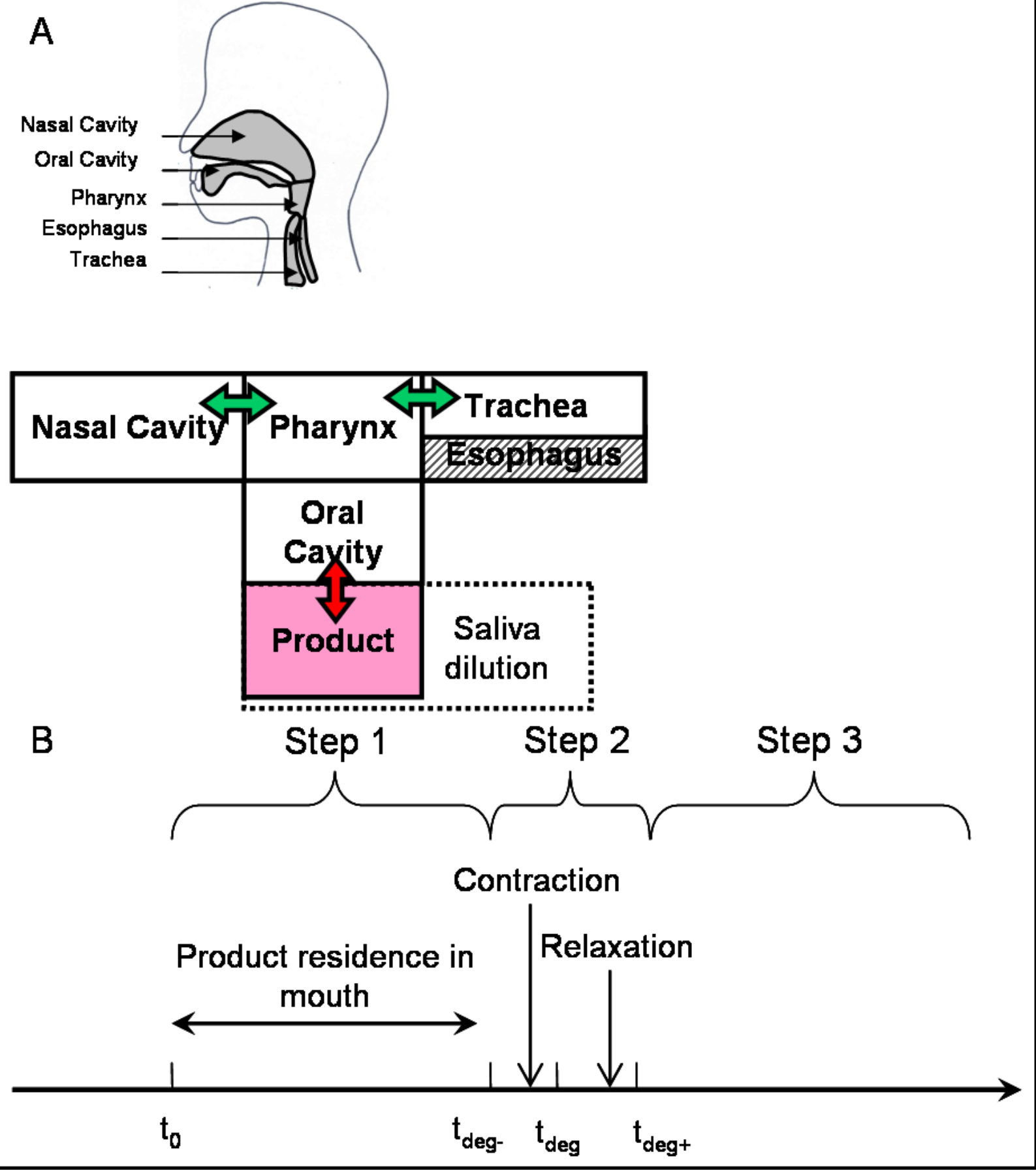
A
Nasal Cavity
Oral Cavity
Pharynx
Esophagus
Trachea
Nasal Cavity
Pharynx
Trachea
Esophagus
Oral Cavity
Product
Saliva dilution
B
Step 1
Step 2
Step 3
Contraction
Relaxation
Product residence in mouth
t_0
t_{deg-}
t_{deg}
t_{deg+}

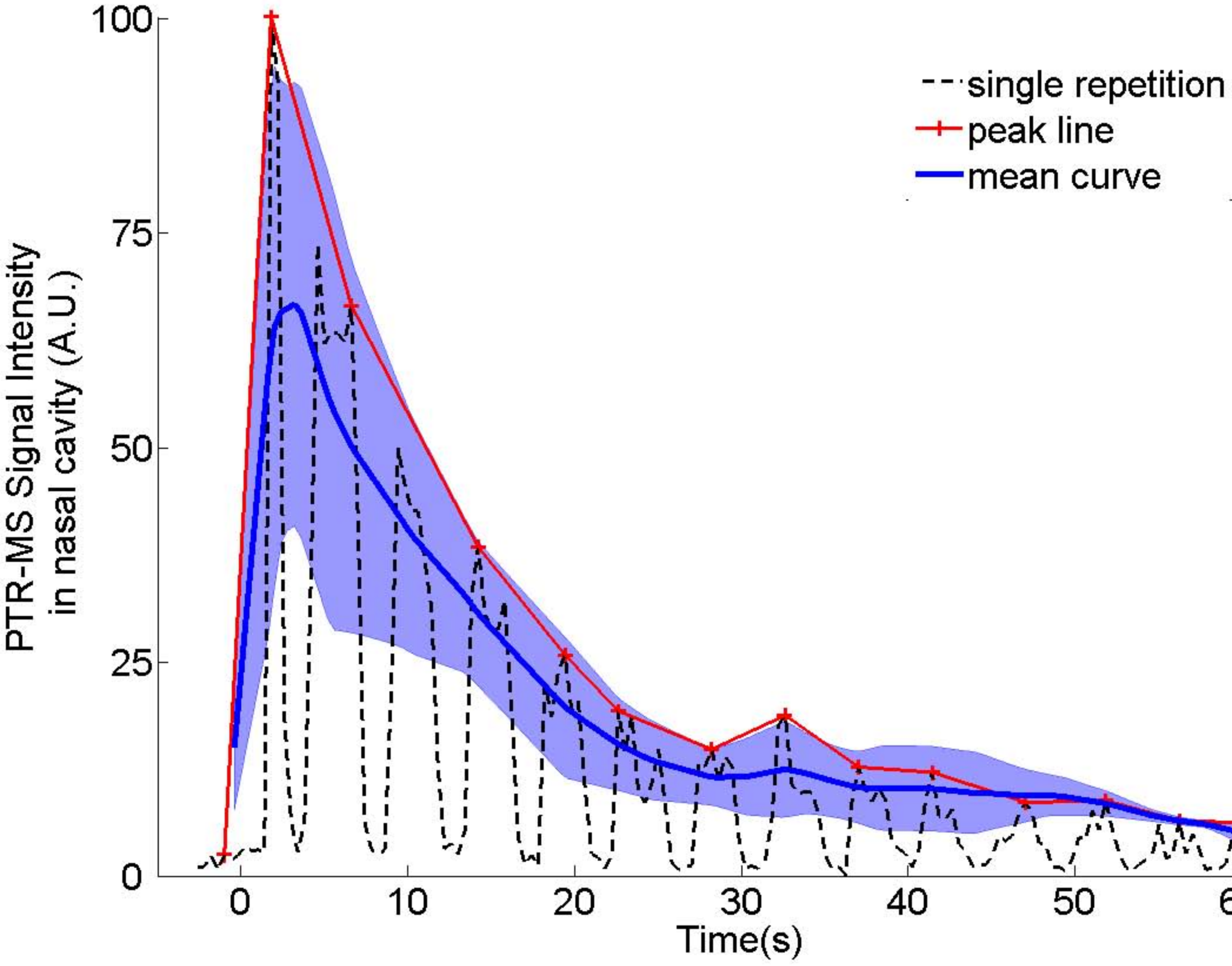
single repetition
peak line
mean curve
PTR-MS Signal Intensity
in nasal cavity (A.U.)
100
75
50
25
0
0
10
20
30
40
50
60
Time(s)

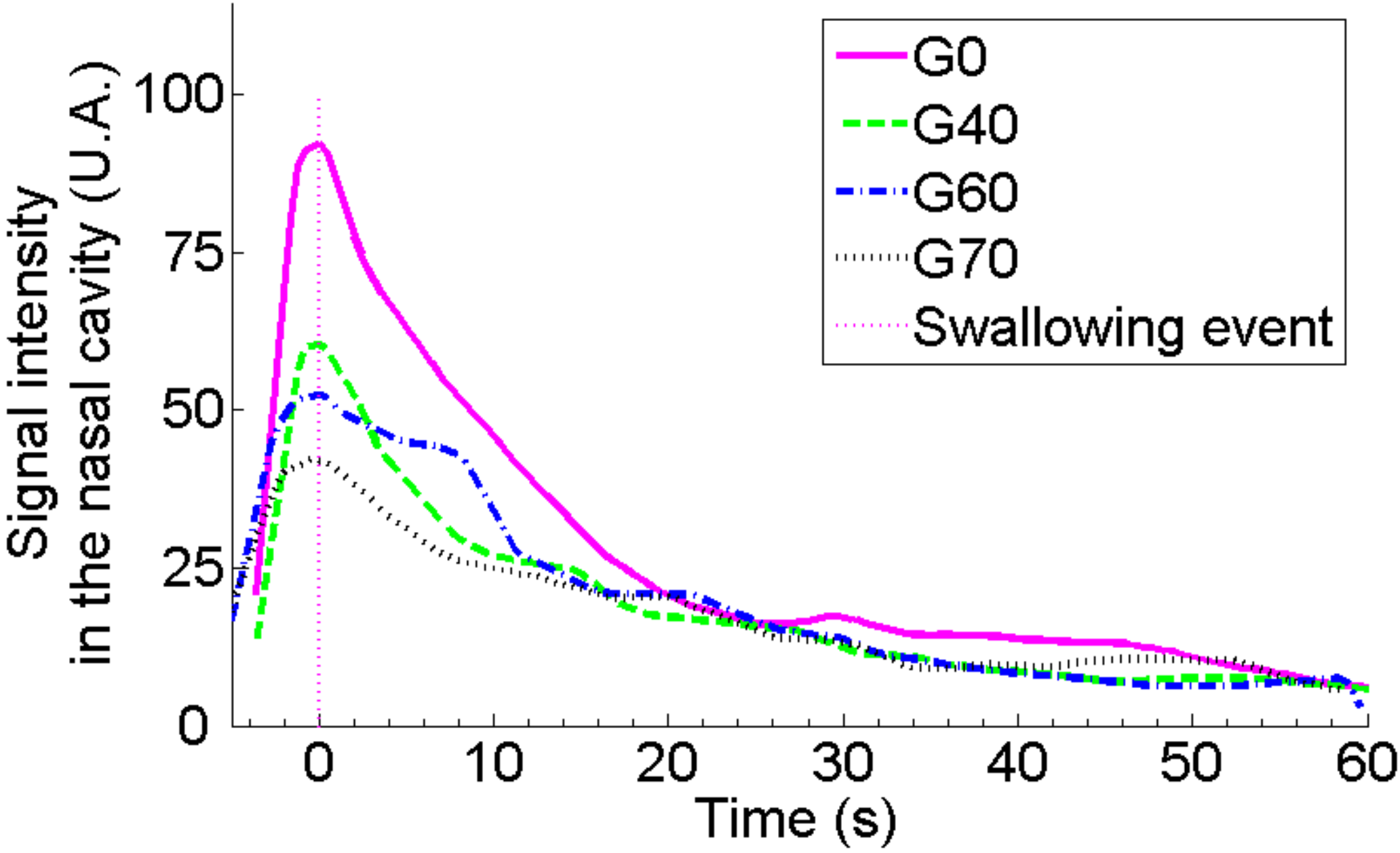
Signal intensity
in the nasal cavity (U.A.)
100
75
50
25
0
0
10
20
30
40
50
60
Time (s)
G0
G40
G60
G70
Swallowing event

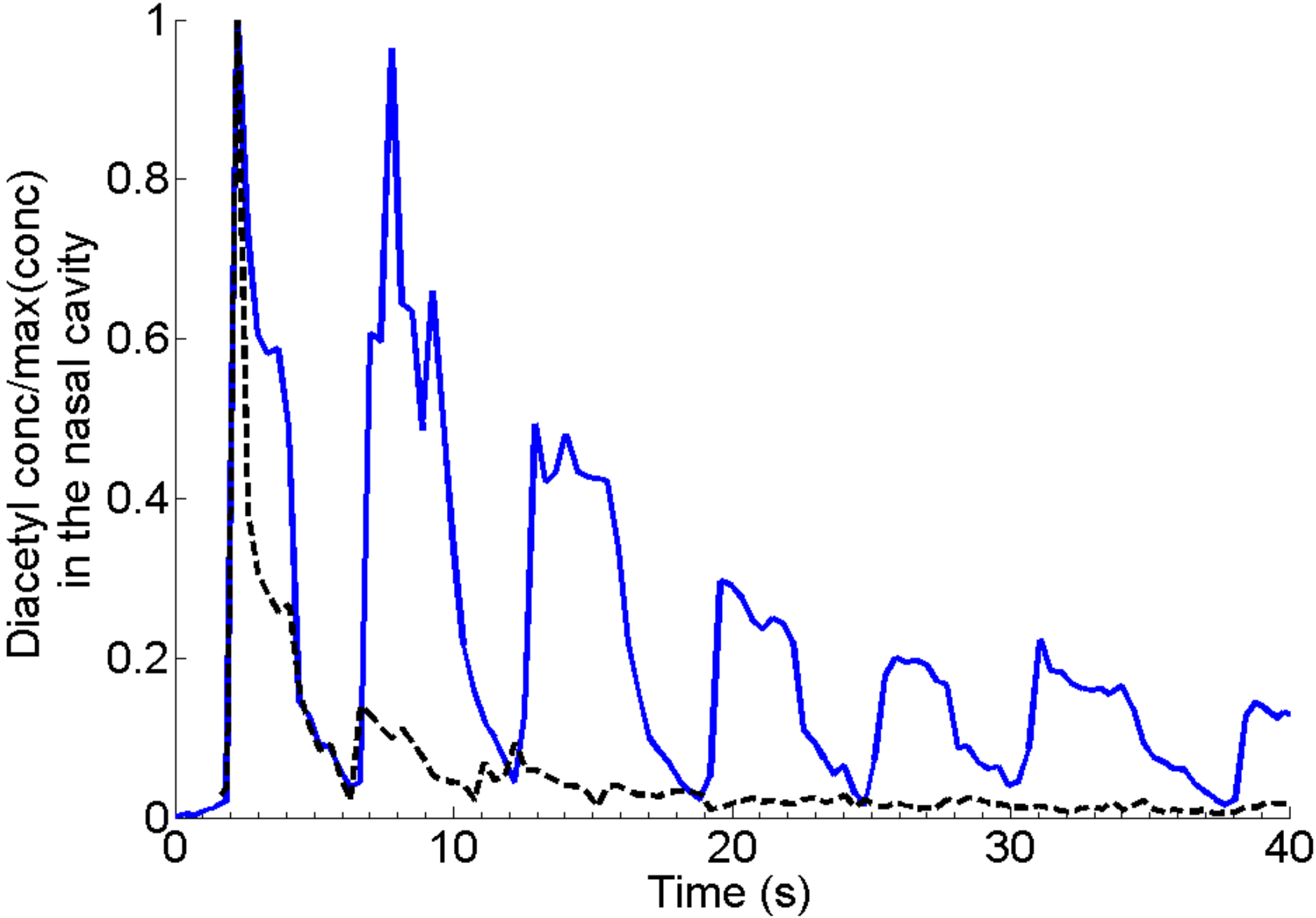
Diacetyl conc/max(conc)
in the nasal cavity
1
0.8
0.6
0.4
0.2
0
0
10
20
30
40
Time (s)

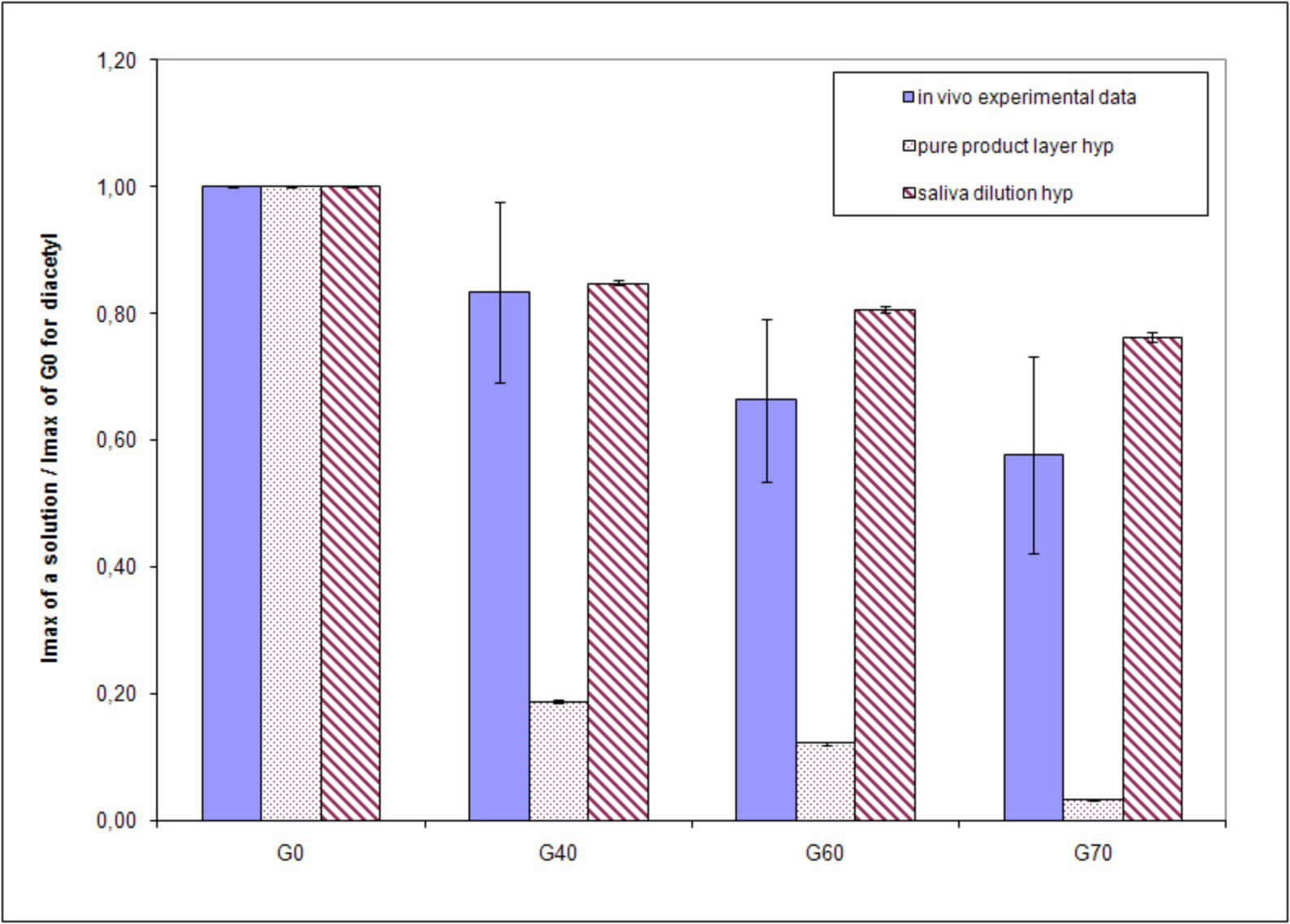
1,20
1,00
0,80
0,60
0,40
0,20
0,00
Imax of a solution / Imax of G0 for diacetyl
in vivo experimental data
pure product layer hyp
saliva dilution hyp
G0
G40
G60
G70

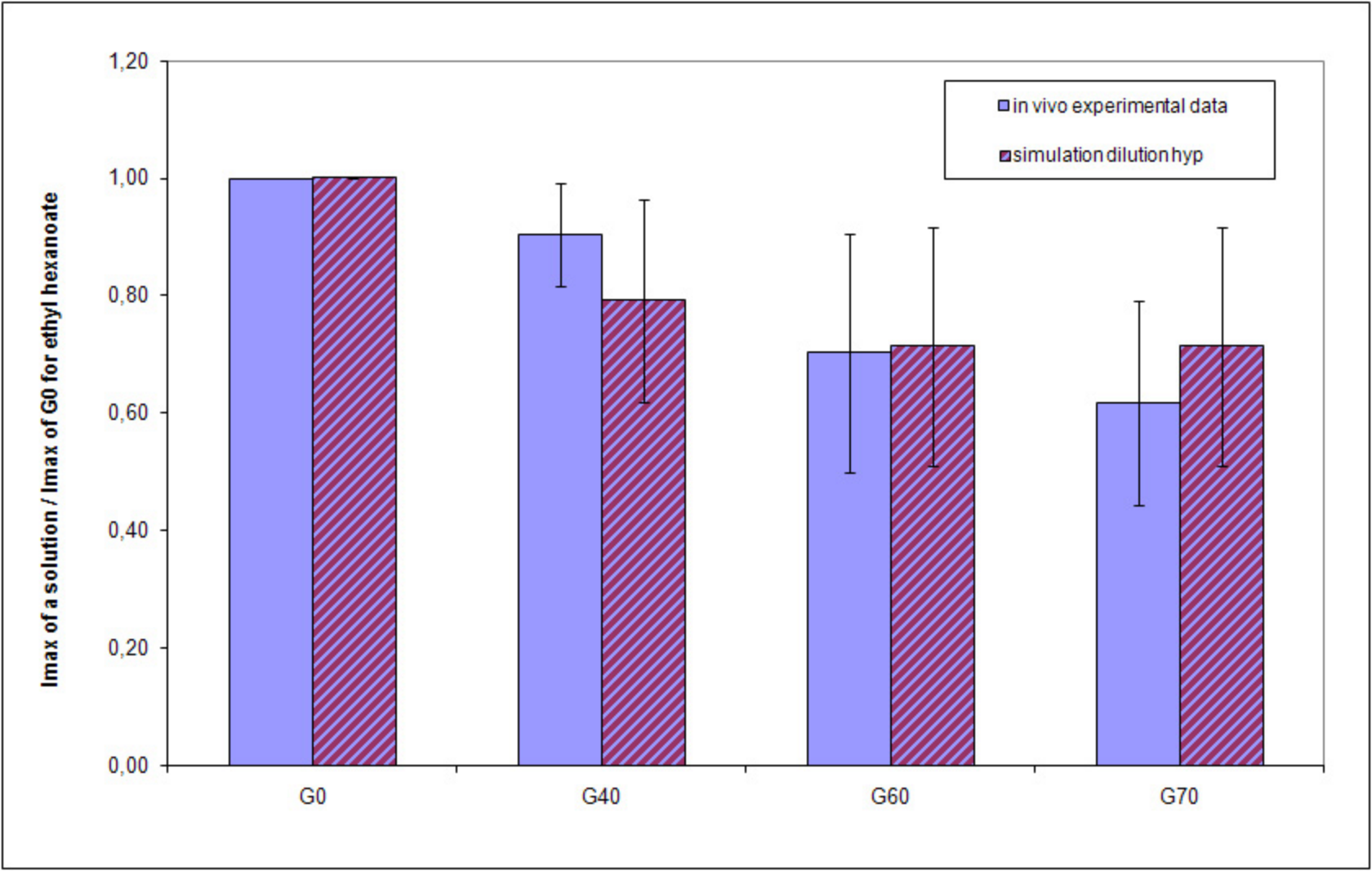
1,20
1,00
0,80
0,60
0,40
0,20
0,00
Imax of a solution / Imax of G0 for ethyl hexanoate
in vivo experimental data
simulation dilution hyp
G0
G40
G60
G70